Controller Design of a Wire-Driven Flexible Robot

MONA TAHMASEBI
Agricultural Engineering Research Department,
Markazi Agricultural and Natural Resources Research and Education Center,
Research, Education and Extension, Organization (AREEO),
Arak, 3818385149,
IRAN

MOHAMMAD GOHARI
Department of Solid Mechanics, Faculty of Mechanical Engineering,
Arak University of Technology,
Arak, 3818146763
IRAN

ABBAS PAK
Department of Mechanical Engineering
Bu-Ali Sina University
Hamedan,
IRAN

Abstract: - Robot tasks and functions are advanced by IoT, remote working, and new human lifestyle requirements in tedious or accurate occupations such as surgery, product inspections, or agriculture harvesting. Numerous robots are technologically advanced by scientists for diverse tasks. Flexible robots are developed based on stated applications since they can adjust their geometry to the working situations. The present study introduces a wire-driven flexible robot stimulated by animal trunks. It can make a motion in planar and space based on the construction of that. Initially, a kinematic model was developed to predict end-effector trajectory, and then a dynamic model was established to compute the required tension of tendon wires based on bending beam theory. Models are simulated by MATLAB/SIMULINK Software and implemented by a generic controller. Various input functions are applied to the model, and outputs show good stability and accuracy. Based on these results, in future work, a WDFR will be developed and controlled by the current presented PID controller.

Key-Words: - Wire Driven Flexible Robot, Dynamic Model, Kinematic Model, Inverse Dynamic, PID Controller

Received: October 23, 2022. Revised: July 8, 2023. Accepted: August 21, 2023. Published: September 20, 2023.

1 Introduction

Recently robotics systems and manipulators have been employed in daily life and industry, especially during pandemic disasters. Three categories of robot arms are generated: continuum, discrete, and serpentine, [1]. Serial links and parallel robots are listed as discrete robots. They include several links and joints to provide motion in the desired workspace with definite payload and accuracy in positioning. They have a limited degree of freedom with big size. Oppositely, continuum robots provide an infinite degree of freedom with compact size although their capacity in payload and accuracy is limited. Thus, they are proper for a confined environment. Nevertheless, their accuracy and payload capacity of them is not as much as rigid manipulators. Reports show that continuum robots are in the primary stage and it is an open area for researchers to develop them for novel applications, [2]. Another kind of robot arm is a serpentine robot with more rigidity while they are more flexible than discrete robots. Many applications are presented for them such as laparoscopic surgery, [3].

Most traditional manipulators are actuated by servo motors in each joint or linear motion motors in prismatic links. In live creatures, rigid bones are

connected to muscles via tendons, [4]. During motion, some flexible muscles are shrieked and others are expanded to generate particular motion in the live organ. This mechanism works by producing bending and many organs of humans do this such as hands, feet, fingers, etc. Thus, most artificial muscles mimic this task to present bending motion. Various solutions are developed to create bending in robot arms: Shape Memory Alloy wires, [5], Piezoelectric Ceramic, [6], Pneumatic Artificial Muscles, [7], and Electro Active Polymers, [8], [9]. SMAs use a two-phase alloy in which the phase is changed by electricity and elongation is created. The response time of SMA is normally slow. PZT ceramics produce mechanical stress and strain by exposing it to electrical signals. They are acting faster than SMAs. EAP response time is desired, but the payload is not very high to lift heavy objects. PAMs provide large amounts of force, but their pressure sources are large and expensive air compressors. They work with expandable air tubes and rounded springs.

Wires and pulleys can be used as tendons which are flexible, lightweight, inexpensive, and strong for large tensile forces, [10]. Wire-driven mechanism is used robot arm, [10], [11], and continuum robot, [12], [13], [14], [15], [16]. Building effective continuum robots is still a challenge, and it is an open area for researchers to make enhanced robots for various purposes, [17]. On the other hand, artificial intelligent control methods were developed for robots and dynamical systems with a large range of variations in working conditions, [18], [19], [20], [21], [22]. Combining AI techniques with WDFR can improve the performance of, particularly in Agribots for spraying or seeding mounting a WDFR can improve their efficiency, [22], [23], [24], [25], [26], [27], [28], [29], [30]. Also, other types of robots such as UAVs can be implemented to this kind of manipulators for various field operations, [30], [31], [32], [33], [34], [35], [36], [37], [38], [39], [40].

Current work aims to present a simulation study on a wire-driven flexible robot based on governed kinematic and dynamic models and design a generic controller based on them.

2 Methodology

Firstly, the kinematic model of the WDFR is explained, and then the dynamic model which is established based on beam theory is mentioned. Besides, the design of a generic controller for feedback control of WDFR is described. By simulation study, the performance of WDFR in positioning and tracking is assessed.

2.1 Kinematic Model of WDFR

The structure of the proposed WDFR consists of ten vertebras in a conical shape. The vertebra as a segment of the kinematic chain is connected to other vertebras. Four wires are passed through each vertebra. This chain is mounted to a base. By applying tension on each cable, bending occurs in the WDFR. Thus, the behavior of WDFR is the same as a cantilever bar exposed to a bending moment. The deflection of the beam provides positioning for the WDFR end effector. Thus, various tensions in the cables generate different bending moments on the cantilever bar. Figure 1 illustrates a schematic structure of WDFR. By bending occurrence, the beam is bent as a part of the arc. Therefore, by employing beam bending theory, the position of the end effector is reached with regard to the curvature created. Figure 2 shows the curvature radius of the cantilever bar as WDFR. This figure illustrates the final shape of the manipulator during bending to reach to target.

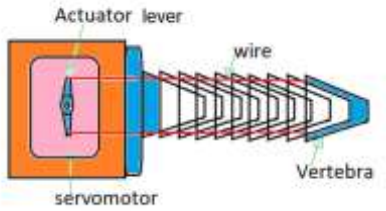

Fig. 1: WDFR components

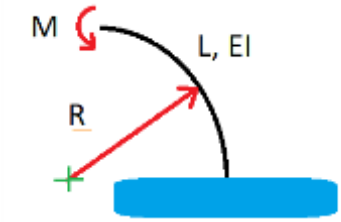

Fig. 2: Curvature radius of cantilever beam

The location of the end effector is presented by P(x,y) in planar Cartesian space, and the radius of curvature is denoted by R. Refer to Figure 3, y can be reached by:

$$y = R - R\cos \propto = R(1 - \cos \propto) \quad (1)$$

And x is calculated by:

$$x = Rsin \propto \quad (2)$$

Where "α" is the axe angle of the created arc. Here, the curvature radius "R" is obtained by the bending moment as:

$$\frac{1}{R} = \frac{M}{EI} \rightarrow R = \frac{EI}{M} \quad (3)$$

Where, E is Young's modulus, and I is the second moment of area of the cantilever bar. To compute M, the dynamic model of WDFR must be presented based on the beam theory.

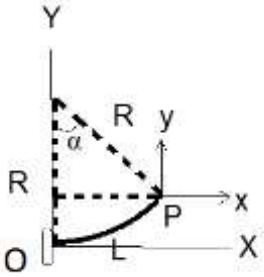

Fig. 3: Position of end effector regarding bending

2.1.1 Dynamic Model of WDFR

Regards to the bent beam theory, the curvature radius can be acquired as:

$$EI\frac{d^2y}{dx^2} = M \quad (4)$$

$$\frac{1}{R} = \frac{d^2y}{dx^2} \quad (5)$$

In addition, the exposed mechanical normal stress due to the tension of the wire is attained by:

$$\sigma = \frac{Mc}{I} \quad (6)$$

The normal stress is gotten by dividing the tension force (F) to cross area (A):

$$\frac{F}{A} = \frac{Mc}{I} \rightarrow M = \frac{IF}{cA} \quad (7)$$

On the other hand, the vertical deflection of the bent beam in the tip of that is calculated by:

$$y = \frac{ML^2}{2EI} \quad (8)$$

Thus, from Eq.7 and 8, "y" is available:

$$y = \frac{FL^2}{2CAE} \quad (9)$$

Consequently, the dynamic model of the WDFR has developed with respect to the identified position from curvature radius and bending moment. Now, the position of the end effector and the needed tension of the wire are presented consequently the design of the controller of the WDFR can be done.

3 Simulation of WDFR

To study the accuracy and stability of the desired controller, a simulation of the WDFR is conducted based on the attained kinematic model and dynamic model. In the first step, a block diagram is constructed in MATLAB/Simulink Software to simulate the position of WDFR `s end effector. Next, a block diagram is developed for the tendon actuator. Figure 4 exemplifies the closed-loop diagram of the designed PID controller. The length of the WDFR is 18cm, and the diameter of the conical components is 3cm.

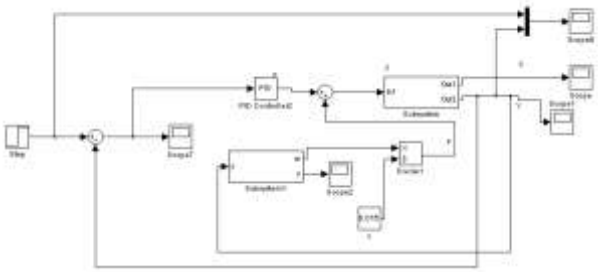

Fig. 4: Block diagram of designed PID controller

The subsystem includes a dynamic model, and subsystem 1 consists of inverse dynamics used in the controller. Equations of the dynamic model are constructed by mathematical operators in the subsystem, and they are shown in Figure 5. The dynamic inverse used in the controller is revealed in Figure 6.

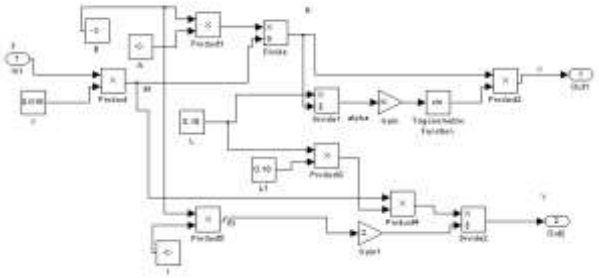

Fig. 5: block diagram of dynamic model based on equation stated

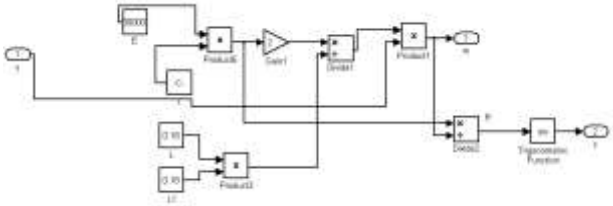

Fig. 6: Dynamic inverse of WDFR shown by block diagram

The step function and ramp function are applied in the system as desired values of end effector height. The output of simulated WDFR is reached to reduce the error between actual output and desired output by tuning the PID. The PID coefficients are obtained as Kp=700, Ki=10, and Kd=0.8. The crude

method is employed for PID tuning. Moreover, the random function is inserted into the WDFR controller because its variation is high, and the output of the system can unveil the robustness of the controller in terms of stability and accuracy.

4 Results and Discussions

The response of the WDFR is reached when the step function is applied to the manipulator. As can be seen in Figure 7, the closeness of output to desired input is very high. The error value is 0.01%. Moreover, the PID presents enhanced performance when a ramp function is considered as input. In this case, the error value is obtained as 0.05%. Next, a random function is imported to the WDFR due to high variations in values. Similar to the mentioned input cases, the WDFR can follow a trajectory with acceptable error and high accuracy. The error value is 0.03%. It is revealed in Figure 8. Also, a random signal is applied as input to the controller, and the response of the robot is very superior. It follows the input signal perfectly. Thus, the accuracy of the WDFR implemented to the PID controller is acquired properly. Lastly, the correlation of WDFR output and random function is presented in Figure 9.

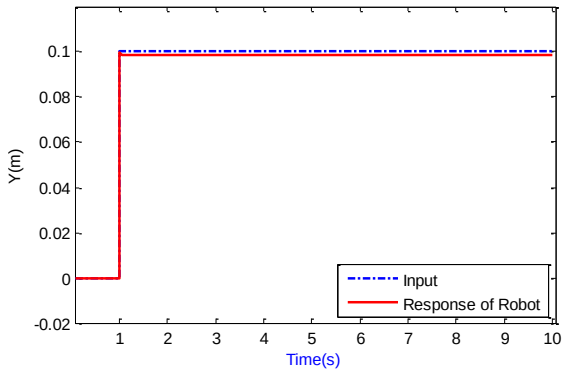

Fig. 7: The WDFR response to step function

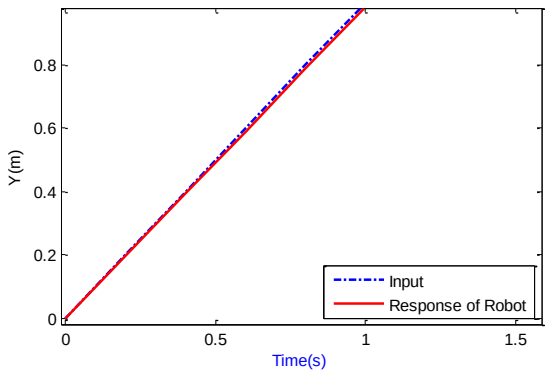

Fig. 8: Convergence between WDFR response and ramp function as desired input

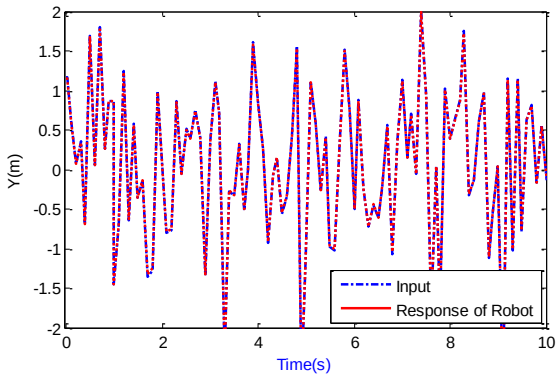

Fig. 9: Correlation of WDFR output and random function

5 Conclusion

Kinematic and Dynamic models of the WDFR are stated, and a simulation study is conducted to evaluate the performance of that when exposed to different desired inputs. The designed PID for WDFR is tuned by the crude method. The results show that the proposed PID provides proper control to the current WDFR in terms of accuracy with minimum error. Consequently, employing a PID controller in this case will be desired and low cost. In future works, based on this achievement, a test rig of WDFR will be introduced and to be used in various operations.

References:

[1] G. Robinson, J. B. C. Davies, "Continuum Robots – a State of the Art," Proceedings of the 1999 IEEE International Conference on Robotics and Automation, pp. 2849-2854, May, 1999.

[2] P. E. Dupont, J. Lock, B. Itkowitz, E. Butler. "Design and Control of Concentric-Tube Robots," IEEE Transactions on Robotics. vol. 26, No. 2, p.209-225, 2010.

[3] W. J. Yoon, P.G. Reinhall, E. J. Seibel, "Analysis of Electro-active Polymer Bending: A Component in a Low-Cost Ultrathin Scanning Endoscope," Sensors and Actuators A: Phys, 133 pp.506-517, 2007.

[4] "Anatomy 12 Wrist and Forearm motions" at: http://www.davidlnelson.md/anatomy13%20Extensor%20 Mechanism.htm

[5] V. D. Sars, S. Hyliyo, J. Szewczyk. "A practical approach to the design and control of active endoscopes", Mechatronics. vol. 20, pp. 251-264, 2010.

[6] T. Idogaki, T. Tominaga, K. Senda, N.Ohya, T. Hattori, "Bending and expanding motion actuators," Sensors and Actuators A: Phys, 54, pp. 760-764, 1996.

[7] B. A. Jones, I. D. Walker, "Kinematics for Multisection Continuum Robots," IEEE Transactions on Robotics, vol. 22, No.1, pp.43-57, Feb. 2006.

[8] C. Laschi, B. Mazzolai, V. Mattoli, M. Cianchetti, P. Dario, "Design of a biomimetic robotic octopus arm," Bioinspiration & Biomimetic, doi: 10.1088/1748-3182/4/1/015006, 2009

[9] C. Laschi, B. Mazzolai, V. Mattoli, M. Cianchetti, P. Dario, "Design and Development of A Soft Actuator for a Robot Inspired By the Octopus Arm" Experimental Robotics: The 11th Intern. Symp. STAR 54, pp. 25-33, 2009

[10] R. Dekker, A. Khajepour, S. Behzadipour, "Design and testing of an ultra-high-speed cable robot," Int. J. of Robotics and Automation, vol. 21, no.1, pp. 25–34, 2006.

[11] S. K. Mustafa, G. J. Yang SH. Yeo, W. Lin, IM. Chen, "Self-Calibration of a Biologically Inspired 7 DOF Cable-Driven Robotic Arm," IEEE/ASME Transactions on mechatronics, vol. 13, No.1, pp. 66-75, Feb. 2008

[12] C. Q. Li, C. D. Rahn, "Design of Continuous Backbone, Cable-Driven Robots", J. of Mechanical Design, vol. 124, pp. 265-271, 2002

[13] K. Xu, N. Simaan, "Analytic Formulation for Kinematics, Statics, and Shape Restoration of Multibackbone Continuum Robots Via Elliptic Integrals," J. of Mechanisms and Robotics, vol. 2, doi: 011006-1 Feb. 2010.

[14] Yeshmukhametov, A., Koganezawa, K., Yamamoto, Y. (2019). A novel discrete wire-driven continuum robot arm with passive sliding disc: Design, kinematics and passive tension control. *Robotics*, *8*(3), 51.

[15] Yeshmukhametov, A., Koganezawa, K., Yamamoto, Y. (2018, December). Design and kinematics of cable-driven continuum robot arm with universal joint backbone. In *2018 IEEE International Conference on Robotics and Biomimetics (ROBIO),* pp. 2444-2449. IEEE.

[16] Gao, Y., Takagi, K., Kato, T., Shono, N., Hata, N. (2019). Continuum robot with follow-the-leader motion for endoscopic third ventriculostomy and tumor biopsy. *IEEE Transactions on Biomedical Engineering*, *67*(2), pp.379-390.

[17] R. J. Webster, B. A. Jones. "Design and Kinematic Modeling of Constant Continuum Robots: A Review," Int. J. of Robotics Research, vol.29, pp. 1661-1683, 2010.

[18] Gohari, M., Abd Rahman, R., Raja, R. I., Tahmasebi, M. (2012, February). Bus seat suspension modification for pregnant women. In 2012 International Conference on Biomedical Engineering (ICoBE), pp. 404-407. IEEE.

[19] Gohari, M., Rahman, R. A., Tahmasebi, M. (2014). Prediction head acceleration from hand and seat vibration via artificial neural network model. In Applied Mechanics and Materials, Vol. 471, pp. 161-166. Trans Tech Publications Ltd.

[20] Gohari, M., Tahmasebi, M., Nozari, A. (2014, October). Application of machine learning for NonHolonomic mobile robot trajectory controlling. In 2014 4th International Conference on Computer and Knowledge Engineering (ICCKE), pp. 42-46. IEEE.

[21] Tahmasebi, M., Gohari, M., Emami, A. (2022). An Autonomous Pesticide Sprayer Robot with a Color-based Vision System. International Journal of Robotics and Control Systems, 2(1), pp.115-123.

[22] Tahmasebi, M., Rahman, R. A., Mailah, M., Gohari, M. (2012). Sprayer boom active suspension using intelligent active force control. Journal of World Academy of Science, Engineering and Technology, 68, pp.1277-1281.

[23] V. Komasilovs, E. Stalidzans, V. Osadcuks, and M. Mednis, "Specification development of robotic system for pesticide spraying in greenhouse," 14th International Symposium on Computational Intelligence and Informatics (CINTI), pp. 453-457, 2013, https://doi.org/10.1109/CINTI.2013.6705239

[24] Y. Sun, S. Zhang, W. Li, "Guidance lane detection for pesticide spraying robot in cotton fields," Journal-Tsinghua University, vol. 47, no. 2, p. 206, 2007, http://en.cnki.com.cn/Article_en/CJFDTotal-QHXB200702011.htm.

[25] D. Deshmukh, D. K. Pratihar, A. K. Deb, H. Ray, N. Bhattacharyya, "Design and Development of Intelligent Pesticide Spraying System for Agricultural Robot," Advances in Intelligent Systems and Computing, pp. 157-170, 2020,

https://doi.org/10.1007/978-3-030-73050-5_16.

[26] N. R. Dhumale, P. C. Bhaskar, "Smart Agricultural Robot for Spraying Pesticide with Image Processing based Disease Classification Technique," International Conference on Emerging Smart Computing and Informatics (ESCI), pp. 604-609, 2021, https://doi.org/10.1109/ESCI50559.2021.9396959.

[27] K. R. Vikram, "Agricultural Robot–A pesticide spraying device," International Journal of Future Generation Communication and Networking, vol. 13, no. 1, 150-160, 2021, https://www.researchgate.net/publication/340827655.

[28] N. S. Bargir, A. S. Vadagaonkar, K. M. Kamble, A. R. Patil, V. Metkari, "Automatic Pesticide Spraying Machine," International Journal of Advance Scientific Research and Engineering Trends, vol. 6, no. 6, 2021, http://www.ijasret.com/VolumeArticles/FullTextPDF/907_20.AUTOMATIC_PESTICIDE_SPRAYIN G_MACHINE.pdf.

[29] A. G. Bhat, "Arecanut Tree-Climbing and Pesticide Spraying Robot using Servo Controlled Nozzle," Global Conference for Advancement in Technology (GCAT), pp. 1-4, 2019, https://doi.org/10.1109/GCAT47503.2019.8978452.

[30] R. G.Wang, H. B. Huang, Y. Li, J. W. Yuan, "Design and Analysis of a Novel Tree Climbing Robot Mechanism," 2020, https://doi.org/10.21203/rs.3.rs-55599/v1.

[23] A. N. Ibrahim, O. Y. Pang, W. K. Yap, and A. S. A. Ghani, "Design of Fast Climbing Robot for Tree with Multiple Diverging Branches," RITA, 395-402, Springer, Singapore, Mechanism, 2018, https://doi.org/10.1007/978-981-13-8323-6_33.

[31] X. Yang, M. Yan, Y. Zhou, R. Liu, "The Dynamic analysis of Planetary roller screw in Tree-climbing robot," Journal of Physics: Conference Series, vol. 2029, no. 1, p. 012060, IOP Publishing, 2021, https://doi.org/10.1088/1742-6596/2029/1/012060.

[32] Z. Yanliang, L. Qi, Z. Wei, "Design and test of a six-rotor unmanned aerial vehicle (UAV) electrostatic spraying system for crop protection," International Journal of Agricultural and Biological Engineering, vol. 10, no. 6, pp. 68-76, 2017, https://doi.org/10.25165/j.ijabe.20171006.3460.

[33] X. Zhou, J. He, D. Chen, J. Li, C. Jiang, M. Ji, M. He, "Human-robot skills transfer interface for UAV-based precision pesticide in dynamic environments," Assembly Automation, 2021, https://doi.org/10.1108/AA-11-2020-0161.

[34] Tahmasebi M., Gohari M., Emami A. "An autonomous pesticide sprayer robot with a color-based vision system," Int. J. Robot. Control Syst, 2022, Vol.2, no.1, p.115-123. http://pubs2.ascee.org/index.php/ijrcs

[35] M. N. Kharim, A. Wayayok, A. R. M. Shariff, A. F. Abdullah, E. M. Husin, "Droplet deposition density of organic liquid fertilizer at low altitude UAV aerial spraying in rice cultivation," Computers and Electronics in Agriculture, vol. 167, p. 105045, 2019, https://doi.org/10.1016/j.compag.2019.105045.

[36] S. Khan, M. Tufail, M. T. Khan, Z. A. Khan, J. Iqbal, A. Wasim, "Real-time recognition of spraying area for UAV sprayers using a deep learning approach," Plos one, vol. 16, no. 4, p. e0249436, 2021, https://doi.org/10.1371/journal.pone.0249436

[37] C.Wang, J. Song, X. He, Z. Wang, S. Wang, Y. Meng, "Effect of flight parameters on distribution characteristics of pesticide spraying droplets deposition of plant-protection unmanned aerial vehicle," Transactions of the Chinese Society of Agricultural Engineering, vol. 33, no. 23, pp. 109-116, 2017, https://www.ingentaconnect.com/content/tcsae/tcsae/2017/00000033/00000023/art00014.

[38] W. Qin, X. Xue, S. Zhang, W. Gu, B. Wang, "Droplet deposition and efficiency of fungicides sprayed with small UAV against wheat powdery mildew," International Journal of Agricultural and Biological Engineering, vol. 11, no. 2, pp. 27-32, 2018, https://doi.org/10.25165/j.ijabe.20181102.3157.

[39] Y. Meng, J. Su, J. Song, W. H. Chen, Y. Lan, "Experimental evaluation of UAV spraying for peach trees of different shapes: Effects of operational parameters on droplet distribution," Computers and Electronics in Agriculture, vol. 170, p. 105282, 2020, https://doi.org/10.1016/j.compag.2020.105282.

[40] M. Gohari, M. Tahmasebi, and M. Sadeghian, "The iterative learning method in NonHolonomic mobile robot," NCMEIS01.

Contribution of Individual Authors to the Creation of a Scientific Article (Ghostwriting Policy)

- Mona Tahmasebi carried out the simulations.
- Mohammad Gohari modelled the robot.
- Abbas Pak fabricated the robot.

Sources of Funding for Research Presented in a Scientific Article or Scientific Article Itself

No funding was received for conducting this study.

Conflict of Interest

The authors have no conflicts of interest to declare.

Creative Commons Attribution License 4.0 (Attribution 4.0 International, CC BY 4.0)

This article is published under the terms of the Creative Commons Attribution License 4.0
https://creativecommons.org/licenses/by/4.0/deed.en_US